

AD-A043 035

ROME AIR DEVELOPMENT CENTER GRIFFISS AFB N Y
REFRACTIVE INDEX CHANGES IN OPTICAL FIBERS SUBJECT TO DIAMETRAL--ETC(U)
APR 77 P D GIANINO, B BENDOW
RADC-TR-77-140

F/G 20/6

UNCLASSIFIED

NL

| OF |

AD
A043035



END
DATE
FILMED
9 -77
DDC

AD A 043035

RADC-TR-77-140
IN-HOUSE REPORT
APRIL 1977

12
B.S.



Refractive Index Changes in Optical Fibers Subject to Diametral Stress

PETER D. GIANINO
BERNARD BENDOW

DDC
RECEIVED
AUG 19 1977
RECEIVED
B

Approved for public release; distribution unlimited.

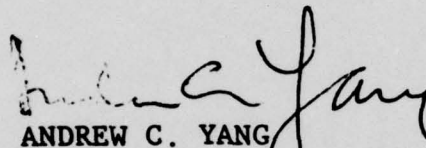
AD No. _____
DDC FILE COPY.

ROME AIR DEVELOPMENT CENTER
AIR FORCE SYSTEMS COMMAND
GRIFFISS AIR FORCE BASE, NEW YORK 13441

This report has been reviewed by the RADC Information Office (OI) and is releasable to the National Technical Information Service (NTIS). At NTIS it will be releasable to the general public, including foreign nations.

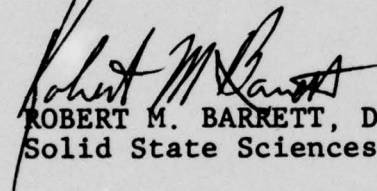
This technical report has been reviewed and approved for publication.

APPROVED:



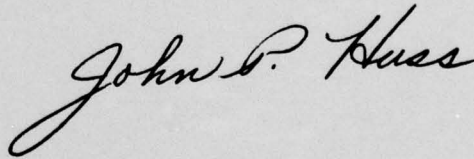
ANDREW C. YANG
Leader,
Electro-Optical Device Technology Program
Solid State Sciences Division

APPROVED:



ROBERT M. BARRETT, Director
Solid State Sciences Division

FOR THE COMMANDER:



Unclassified

SECURITY CLASSIFICATION OF THIS PAGE (When Data Entered)

REPORT DOCUMENTATION PAGE		READ INSTRUCTIONS BEFORE COMPLETING FORM	
1. REPORT NUMBER RADC-TR-77-140	2. GOVT ACCESSION NO.	3. RECIPIENT'S CATALOG NUMBER <i>Technical report</i>	
4. TITLE (and Subtitle) REFRACTIVE INDEX CHANGES IN OPTICAL FIBERS SUBJECT TO DIAMETRAL STRESS.		5. TYPE OF REPORT & PERIOD COVERED In-House	
6. AUTHOR(s) Peter D. Gianino Bernard Bendow		6. PERFORMING ORG. REPORT NUMBER	
7. PERFORMING ORGANIZATION NAME AND ADDRESS Deputy for Electronic Technology (RADC/ETSS) Hanscom AFB Massachusetts 01731		8. CONTRACT OR GRANT NUMBER(s)	
9. CONTROLLING OFFICE NAME AND ADDRESS Deputy for Electronic Technology (RADC/ETSS) Hanscom AFB Massachusetts 01731		10. PROGRAM ELEMENT, PROJECT, TASK AREA & WORK UNIT NUMBERS 61102F 2304J101	
11. MONITORING AGENCY NAME & ADDRESS (if different from Controlling Office) <i>12/17 p.</i>		12. REPORT DATE Apr 10 1977	
13. DISTRIBUTION STATEMENT (of this Report) Recommended for public release; distribution unlimited.		13. NUMBER OF PAGES 19	
14. DISTRIBUTION STATEMENT (of the abstract entered in Block 20, if different from Report)		14. SECURITY CLASS. (of this report) Unclassified	
15. SUPPLEMENTARY NOTES		15a. DECLASSIFICATION/DOWNGRADING SCHEDULE	
16. KEY WORDS (Continue on reverse side if necessary and identify by block number) Photoelasticity Fiber optics Optical fibers Stress		16. DISTRIBUTION STATEMENT A Approved for public release; Distribution Unlimited	
17. ABSTRACT (Continue on reverse side if necessary and identify by block number) We describe the changes in refractive index induced by the photoelastic effect when an optical fiber is subjected to a uniformly applied diametral stress. For easily achievable values of the force per unit length applied to the fiber, we find that regions of equal or higher refractive index than the core may be induced in the outer region of the fiber. Thus the stressed region is capable of acting as a mode converter that affects the transmission characteristics of the fiber.		17. DISTRIBUTION STATEMENT A Approved for public release; Distribution Unlimited	

DD FORM 1 JAN 73 1473 EDITION OF 1 NOV 65 IS OBSOLETE

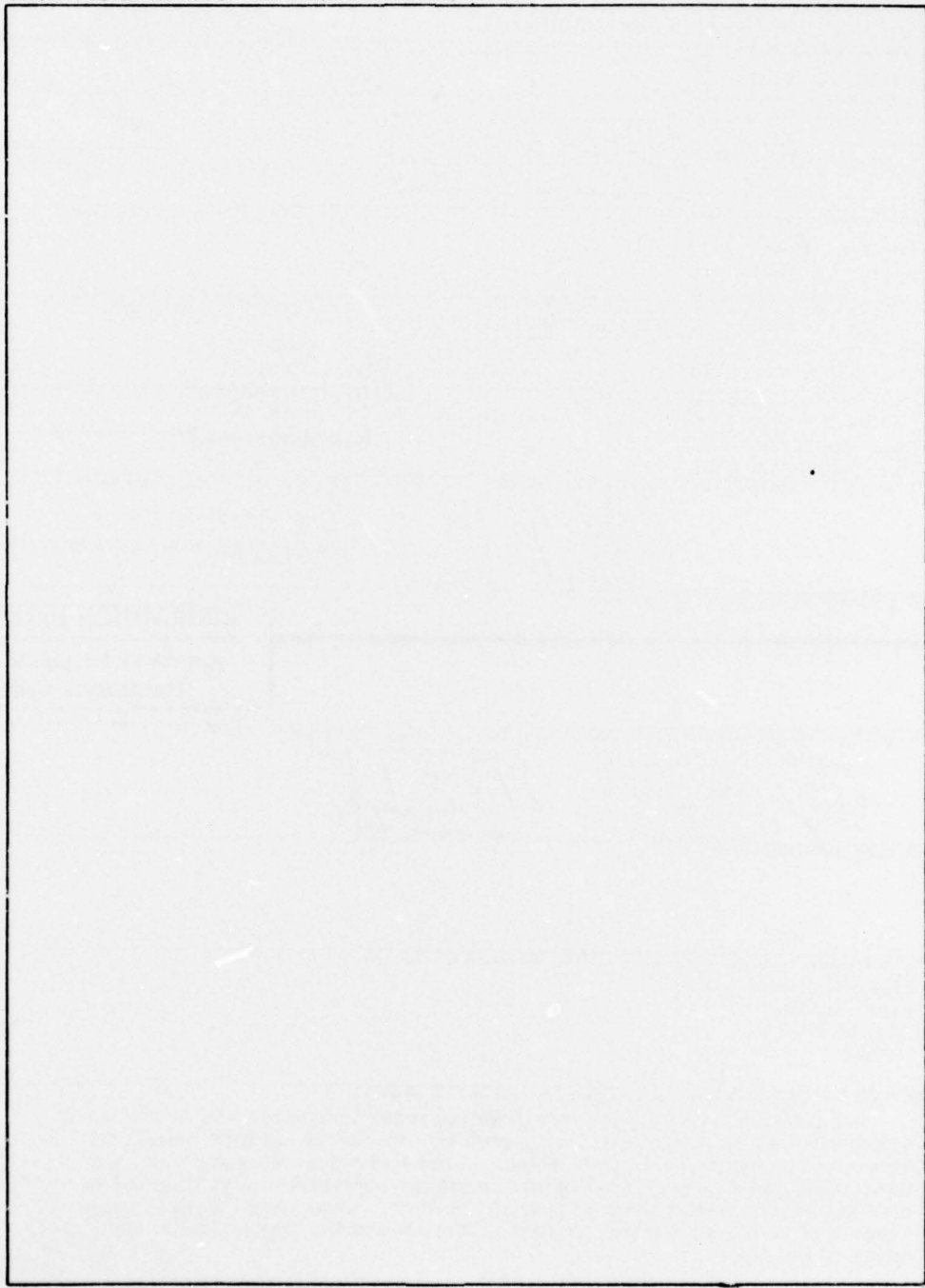
Unclassified

SECURITY CLASSIFICATION OF THIS PAGE (When Data Entered)

* as described.
 ** It was found
 309050

Y/B

SECURITY CLASSIFICATION OF THIS PAGE(When Data Entered)



SECURITY CLASSIFICATION OF THIS PAGE(When Data Entered)

ACCESSION for	
NTIS	White Section <input checked="" type="checkbox"/>
DDC	Buff Section <input type="checkbox"/>
UNANNOUNCED	<input type="checkbox"/>
JUSTIFICATION	
BY	
DISTRIBUTION/AVAILABILITY CODES	
Dist.	AVAIL. and/or SPECIAL
A	

DDC
RECEIVED
 AUG 19 1977
RECEIVED
B

Contents

1. INTRODUCTION	5
2. STRESS-INDUCED CHANGES IN REFRACTIVE INDEX	6
3. CONCLUSIONS	13
APPENDIX A: Fused Silica Parameters Pertinent to Photoelasticity	15
APPENDIX B: Calculation of Strains	17

Illustrations

1. Coordinate System for the Fiber	7
2. Stresses in Fiber	8
3. Stress Differences in Fiber	10
4. Refractive Index Change vs Distance	11
5. Total Refractive Index Change vs Force Applied (F/L) at the Fiber Center (0, 0) and at the Point of Maximum Stress (0, $\pm y_M$)	12

Tables

1. Refractive Index Change vs Force Applied	12
---	----

Refractive Index Changes in Optical Fibers Subject to Diametral Stress

1. INTRODUCTION

When an optical fiber is subjected to a uniform* stress applied along its diameter, refractive index changes will be induced owing to photoelasticity. This phenomenon, one of several which can alter the transmission through optical fibers, may be involved in the observed changes of the transmitted mode patterns in experiments conducted at Solid State Sciences Division (ETSS).† Assuming that a uniform stress is applied to a perfect fiber, one may also induce changes in the geometrical cross section. In the nonuniform case, which may be closer to reality in practice, one may induce microbending and inhomogeneously stressed regions, both of which are capable of altering optical transmission. The present work is limited to an examination of the changes in refractive index and, hence, the waveguiding characteristics of a fiber, induced by the photoelastic effect.

(Received for publication 19 April 1977)

*The term uniform is used in the sense of how the external force is applied and the geometrical shape of the fiber.

†The authors thank Dr. R. Payne for discussions of his experimental results.

2. STRESS-INDUCED CHANGES IN REFRACTIVE INDEX

Whenever an optical medium is stressed, its refractive index becomes altered, a phenomenon which is termed the photoelastic effect. If we represent the refractive index by n , the stress by σ , and the Pockels piezooptic constants by q , then the change in reciprocal of the refractive index squared is given as:¹

$$\Delta(1/n^2)_k = \frac{-2}{n_0^3} \Delta n_k = q_{kj} \sigma_j \quad (k, j = 1, \dots, 6) \quad (1)$$

where the standard (Voigt) compact-subscript notation is used, and n_0 is the refractive index of the unperturbed medium.

Let us set up a coordinate system such that the z -axis is parallel to the cylindrical guide axis, the y -axis parallel to the direction along which opposing external diametral forces are applied, and the origin $x = y = 0$ is located at the center of the guide. The forces (F) extend for a specified length (L) along the z -axis (see Figure 1a). With this setup, any arbitrary point (x, y) in the fiber experiences tensile or compressive stresses parallel to the x - and y -axes (represented by σ_1 and σ_2 , respectively, and shown in Figure 1b) and shear stresses σ_6 ($\equiv \sigma_{xy}$) which tend to cause rotation about the z -axis. However, this latter stress vanishes on the x - and y -axes. Under these circumstances, the total fractional change in refractive index due to the stress at the point (x, y) is given by:

$$\left(\frac{\Delta n}{n}\right)^S = \left(\frac{\Delta n_x}{n}\right)^S - \left(\frac{\Delta n_y}{n}\right)^S = \frac{-n_0^2}{2} (q_{11} - q_{12})(\sigma_1 - \sigma_2)_{x, y} \quad (2)$$

for an optically isotropic material. We initially assume that the force F is applied at the fiber's surface by knife edges running parallel to the z -axis for a length L .

The general expressions for the quantities $(\sigma_1)_{x, y}$ and $(\sigma_2)_{x, y}$ at any arbitrary point (x, y) are derived by Frocht.² Along the x -axis they are given by:

$$(\sigma_1)_{x, 0} = H \left[\frac{D^2 - 4x^2}{D^2 + 4x^2} \right]^2 \quad (3)$$

1. Nye, J. F. (1957) Physical Properties of Crystals, Oxford Press, London, p. 224.

2. Frocht, M. (1948) Photoelasticity, Vol. 2, Wiley, New York, pp. 125-129.

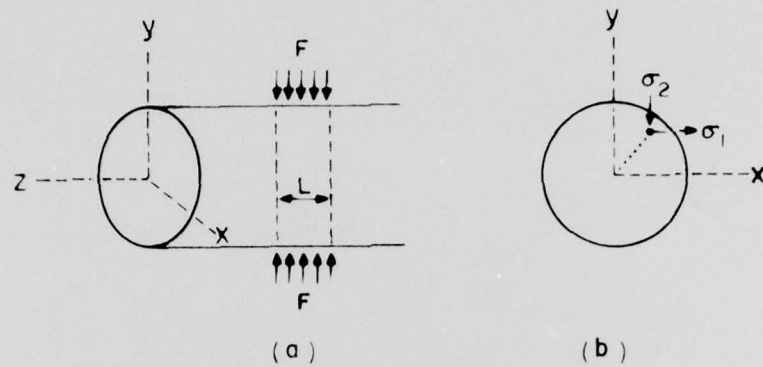


Figure 1. Coordinate System for the Fiber, Showing the Applied External Forces (F) and the Resulting Internal Stresses (σ) at an Arbitrary Point

$$(\sigma_2)_{x,0} = -H \left[\frac{4 D^4}{(D^2 + 4 x^2)^2} - 1 \right]$$

where D is the fiber diameter, the range of x is $0 \leq |x| \leq |D/2|$, and, the quantity H is defined as:

$$H = \left(\frac{2}{\pi D} \right) \frac{F}{L} \quad (5)$$

Along the y -axis ($0 \leq |y| \leq |D/2|$), these two stresses become:

$$(\sigma_1)_{0,y} = H \quad (6)$$

$$(\sigma_2)_{0,y} = -HD \left[\frac{2}{D - 2y} + \frac{2}{D + 2y} - \frac{1}{D} \right] \quad (7)$$

The negative signs in the σ 's indicate that they are compressive stress. The approximate behavior of Eqs. (3), (4), (6) and (7) is shown in Figure 2. These curves are, of course, symmetrical about the origin. On each plot the positive vertical axes pertain to σ_1 , whereas the negative vertical axes refer to σ_2 . Note that the $(\sigma_2)_{0,y}$ curve in Figure 2b becomes infinite at the endpoints ($y = \pm D/2$). This occurs because the force is being applied over an infinitesimally small surface area.

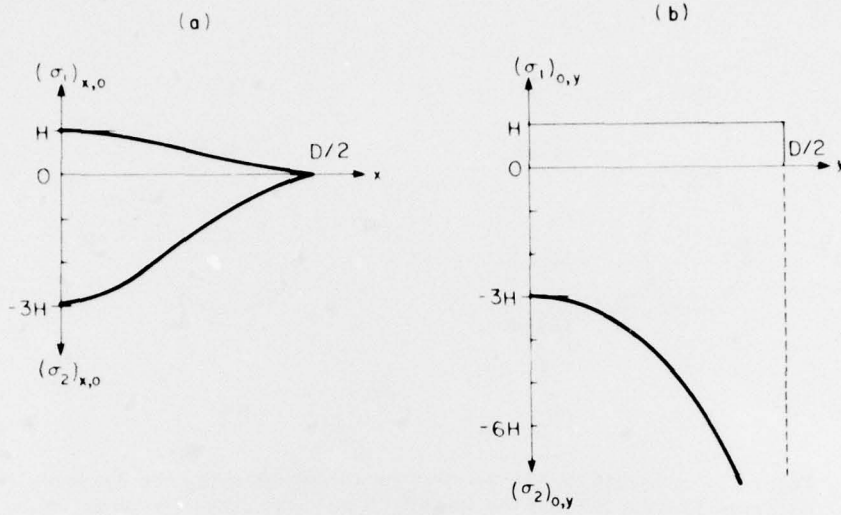


Figure 2. Stresses in Fiber. σ_1 and σ_2 vs distance along the horizontal (x) axis and vertical (y) axis measured from the fiber's center

When the foregoing information is substituted into Eq. (2), we get, after interchanging q_{12} with q_{11} :

$$\left(\frac{\Delta n}{n}\right)_{x,0}^S = \frac{n_o^2}{2} (q_{12} - q_{11})(\sigma_1 - \sigma_2)_{x,0} = \frac{n_o^2}{2} (q_{12} - q_{11}) \{4 HD^2(D^2 - 4x^2)/(D^2 + 4x^2)^2\}, \quad (8)$$

and

$$\left(\frac{\Delta n}{n}\right)_{0,y}^S = \frac{n_o^2}{2} (q_{12} - q_{11})(\sigma_1 - \sigma_2)_{0,y} = \frac{n_o^2}{2} (q_{12} - q_{11}) \{4 HD^2/(D^2 - 4y^2)\}. \quad (9)$$

At the center of the cylinder ($x = y = 0$), both of the preceding equations reduce to:

$$\begin{aligned} \left(\frac{\Delta n}{n}\right)_{0,0}^S &= \frac{n_o^2}{2} (q_{12} - q_{11})(\sigma_1 - \sigma_2)_{0,0} = \frac{n_o^2}{2} (q_{12} - q_{11}) \{4H\} \\ &= n_o^2 (q_{12} - q_{11}) \left\{ \frac{4}{\pi D} \cdot \frac{F}{L} \right\}. \quad (10) \end{aligned}$$

Equation (8) shows that $(\Delta n/n)_{x,0}^S$ has its maximum value at $x = 0$, diminishes with x in almost the same manner as Eq. (3) (see also Figure 2a), then vanishes at $x = \pm D/2$. On the other hand, Eq. (9) behaves quite similarly to Eq. (7) for changing y , including the singularity at the endpoints.

However, if F is applied by means of flat plates, rather than knife-edges, so that the force is distributed over more of the fiber's surface, then the points of maximum stress move a short distance away from the edges, closer to the fiber's center.³ We designate the positions of these points by $\pm y_M$. Since the force-per-unit length employed in our case is of the same order of magnitude as in the example treated by Frocht,³ we should expect similar qualitative results, namely, that the maximum stresses along the y -axis move to a position approximately $\pm D/50$ away from the edge and that the quantity $(\sigma_1 - \sigma_2)_{0,y_M}$ be approximately ten times greater than that at the center, that is,

$$(\sigma_1 - \sigma_2)_{0,y_M} \approx 10 (\sigma_1 - \sigma_2)_{0,0} \quad (11)$$

As a consequence,

$$\left(\frac{\Delta n}{n}\right)_{0,y_M}^S \approx 10 \left(\frac{\Delta n}{n}\right)_{0,0}^S \quad (12)$$

At the edges ($y = \pm D/2$), the magnitude of $(\sigma_1 - \sigma_2)_{0,D/2}$ and $(\Delta n/n)_{0,D/2}^S$ then fall to approximately three times the corresponding values at the center of the fiber.

The term $(\sigma_1 - \sigma_2)_{x,0}$ is plotted in Figure 3a as a function of x . It is given by the quantity inside the curly braces on the right-hand side of Eq. (8). As stated previously, it behaves somewhat like the $(\sigma_1)_{x,0}$ curve of Figure 2a. In Figure 3b, however, we have plotted two versions of the quantity $(\sigma_1 - \sigma_2)_{0,y}$. The solid curve pertains to the case in which the forces are applied by knife-edges. It is governed by the term inside the curly braces on the right-hand side of Eq. (9). The dashed curve pertains to the case in which the forces are applied by flat plates. In accordance with Frocht,³ the profiles for both cases have the same magnitude, namely, $4H$, at the center and behave identically out to a distance of about $D/10$ from the edges. Thereupon, the dashed curve peaks at a value ~ 10 times that at the center ($\sim 40H$) at a point $\sim D/50$ from the edges and then falls to $\sim 12H$ at the edges.

3. See Ref. 2, pp. 27-29.

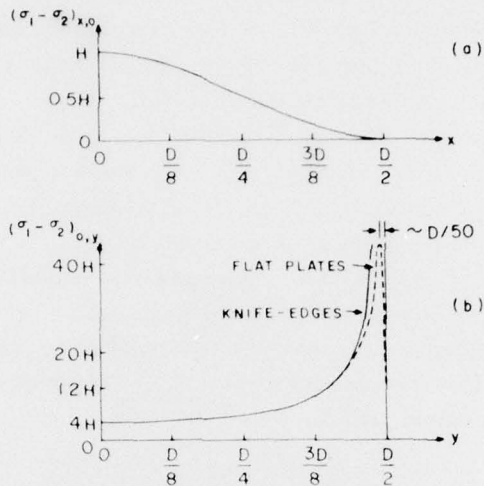


Figure 3. Stress Differences in Fiber. $(\sigma_1 - \sigma_2)$ vs distance along x- and y-axes. The solid curves pertain to application of forces via knife-edges; the dashed curve in (b) via flat plates.

We now particularize our treatment to the case of a fiber having an outer diameter (D) of 5 mils and a core diameter of 3 mils. [For this fiber we get $H = 127 \text{ F/L (lb/in}^2\text{)}$ from Eq. (5).] The fiber is assumed to have a stepped index profile in the unstressed state, the difference in indices between core and cladding being 1 percent. Designating this unstressed refractive index change by $(\Delta n/n)^U$, we plot this versus distance along any arbitrary diameter in Figure 4a.

If we assume that the fiber core is fused silica, then $n_o = 1.5$ and $q_{12} - q_{11} \approx 2 \times 10^{-8} \text{ in}^2/\text{lb}$ (see Ref. 4). If we consider the case in which the forces are applied by means of flat plates, then we could calculate the specific values of $(\Delta n/n)^S$ along the x-axis via Eq. (8) and along the y-axis, using Eqs. (10) and (12), filling in the rest of the values by utilizing the information given previously. (See, for example, the information contained in Figure 3b.) The total refractive index change, designated by $(\Delta n/n)^T_{x,y}$, would then be given by the sum:

$$(\Delta n/n)^T_{x,y} = (\Delta n/n)^U_{x,y} + (\Delta n/n)^S_{x,y} \quad (13)$$

4. Kapron, F. (1952) Birefringence in dielectric optical waveguides, IEEE J. of Q. Elect. QE-8:224.

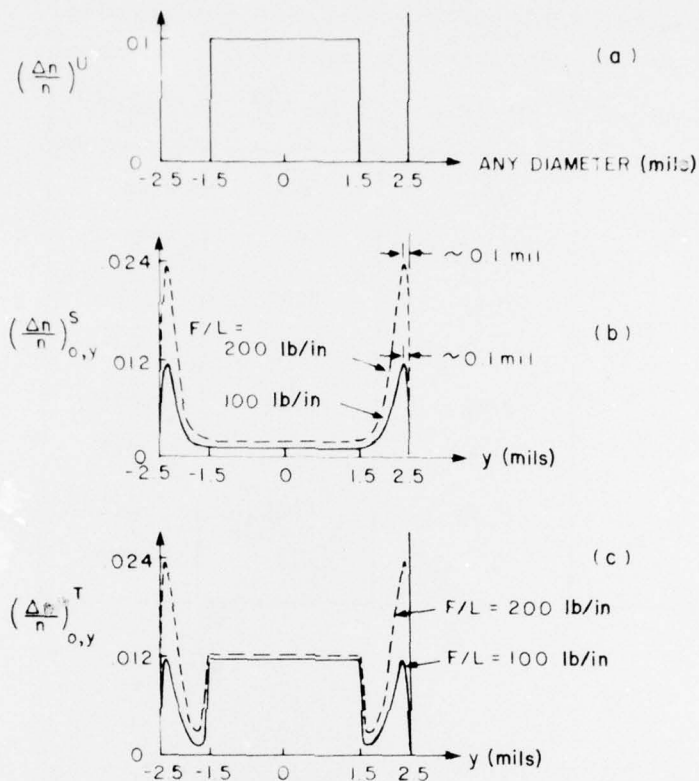


Figure 4. Refractive Index Change vs Distance: (a) unstressed case; (b) stress alone; and (c) total effect

In Table 1 we list the $(\Delta n/n)^S$ and $(\Delta n/n)^T$ for the above silica fiber at 3 locations, namely, the center and the two symmetrical points $(0, \pm y_M)$, for various values of F/L . [Note that $(\Delta n/n)^U$ is always 0.01 at the center and zero at the points $(0, \pm y_M)$].

In Figures 4b and c we utilize some of the information contained in Table 1. In these two figures, we plot the index changes due to stress alone and the total effect, respectively, along the y -axis for $F/L = 100$ and 200 lb/in. Some of the important features of the curves in Figure 4c are brought out much more vividly in Figure 5. Here, we have plotted the total index change as a function of F/L for 3 positions in the fiber, namely, $(0, 0)$ and $(0, \pm y_M)$. Note how the total index change at the center barely increases in magnitude with change of applied F/L . On the other hand, the total index change at the point of maximum stress turns out to be a very sensitive function of F/L . At $F/L = 50$ lb/in, its magnitude is slightly greater than half that at the fiber's center; at 100 lb/in, it is approximately the same; while at 200 lb/in., it becomes almost twice that at the center.

Table 1. Refractive Index Change vs. Force Applied

$\frac{F}{L}$ (lb/in)	Position	$(\Delta n/n)^S$	$(\Delta n/n)^T$
0	(0, 0)	0	.01
	(0, $\pm y_M$)	0	0
50	(0, 0)	.0006	.0106
	(0, $\pm y_M$)	.006	.006
100	(0, 0)	.0011	.0111
	(0, $\pm y_M$)	.011	.011
200	(0, 0)	.0023	.0123
	(0, $\pm y_M$)	.023	.023

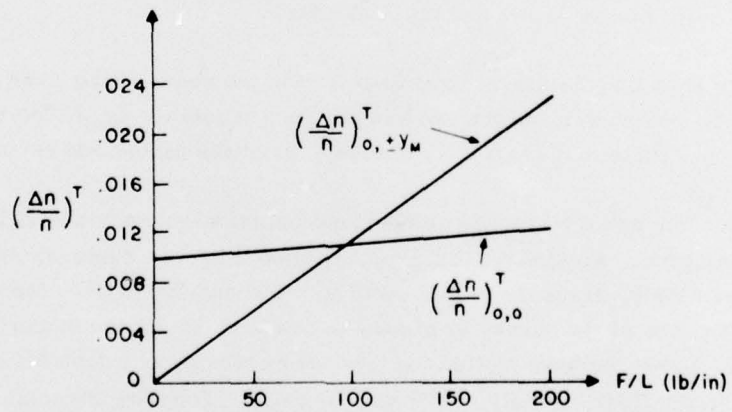


Figure 5. Total Refractive Index Change vs Force Applied (F/L) at the Fiber Center (0, 0) and at the Point of Maximum Stress (0, $\pm y_M$)

It should be remembered that the results displayed in Figures 4b, 4c and 5 hold only along the y-axis. As can be seen with the help of Eq. (8) [and Figure 3a] the $(\Delta n/n)^S$ profile along the x-axis shows a maximum at (0, 0) and drops off to zero at the periphery ($x = \pm D/2$). However, even this maximum is still one order of magnitude lower than the original value of $(\Delta n/n)^U \sim 0.01$. Consequently, the contribution to $\Delta n/n$ along the x-axis due to the stress is unimportant and its total index profile would still be given as shown in Figure 4a. For diametral lines at arbitrary angles with respect to the x- and y-axes, the $(\Delta n/n)^T$ profiles would be somewhere between those shown in Figures 4a and c.

When the applied linear forces are such as to cause large index changes, as shown in Figure 4c, for example, then one must take into consideration the possibility of coupling at least some of the optical signal from the core to the high index region near the periphery. The net effect of this would be the conversion of modes in the core to the stressed region, coupling of energy out of the guide, and deterioration of the original signal. This process of optical coupling would be analogous to quantum mechanical tunneling between two potential wells separated by a barrier.

As a convenience for the reader, we have included two appendices. In Appendix A we list the material parameters for fused silica which would be appropriate for photoelastic analyses. In Appendix B we have calculated the strains at the points (0, 0), $(0, \pm y_M)$, $(0, \pm D/2)$ and $(\pm D/2, 0)$ for the particular fiber treated in this paper.

3. CONCLUSIONS

We have shown that a fiber subjected to easily achievable values of applied stress will assume a refractive index distribution in which portions of the outer region (usually the cladding) possess an equal or greater refractive index than that of the active waveguiding region (core). Hence, the stressed region is capable of supporting new modes and thereby altering the distribution of the old ones; that is, it is capable of acting as a mode mixer or converter. The internal stresses generated by the applied force are typically an order of magnitude or more smaller than those corresponding to the intrinsic strength of fused silica. Although a detailed calculation of the mode conversion induced by transmission through the stressed region would be prohibitively difficult, it nevertheless appears safe to conclude that the mechanism described here can lead to perceptible changes in fiber transmission.

Appendix A

Fused Silica Parameters Pertinent to Photoelasticity

The following quantities are taken from the AIP Handbook¹ and converted into English units:

$$E = \text{Young's Modulus} = 1.06 \times 10^7 \text{ lb/in}^2$$

$$\nu = \text{Poisson ratio} = 0.17$$

$$\mu = \text{Lame's Constant} = .453 \times 10^7 \text{ lb/in}^2$$

$$\lambda = \text{Lame's Constant} = .234 \times 10^7 \text{ lb/in}^2$$

The values of Pockels elastooptic coefficients are taken from Pinnow²

$$p_{11} = .121$$

$$p_{12} = .270$$

The following values of elastic compliances (s_{ij}), stiffness constants (c_{ij}) and Pockels piezooptic coefficients (q_{ij}) are computed from the above quantities:

1. Gray, D.E., Ed. (1972) AIP Handbook, 3rd ed., McGraw-Hill, New York, p 3-104.
2. Pinnow, D.A. (1972) Electro-optic materials, in Laser Handbook, Vol. 1, F. Arecchi and E. Schulz-Dubois, Ed., North Holland Publ. Co., Amsterdam, p. 999.

$$\left. \begin{array}{l} s_{11} = .95 \\ s_{12} = -.16 \\ s_{44} = 2.21 \end{array} \right\} \times 10^{-7} \text{ in}^2/\text{lb}$$

$$\left. \begin{array}{l} c_{11} = 1.14 \\ c_{12} = .23 \\ c_{44} = .45 \end{array} \right\} \times 10^7 \text{ lb/in}^2$$

$$\left. \begin{array}{l} q_{11} = .27 \\ q_{12} = 1.9 \end{array} \right\} \times 10^{-8} \text{ in}^2/\text{lb}$$

Appendix B

Calculation of Strains

Strains (ϵ_j) are related to stresses (σ_i) in a material medium via the elastic compliances (s_{ij}) in the following manner:

$$\epsilon_i = s_{ij} \sigma_j \quad (i, j = 1, \dots, 6) \quad .$$

Again, the compact subscript notation has been employed. However, along the x- and y-axes, only σ_1 and σ_2 exist. Hence, the x- and y- components of strain along these axes in an isotropic material can be written as:

$$\epsilon_1 = s_{11} \sigma_1 + s_{12} \sigma_2$$

$$\epsilon_2 = s_{12} \sigma_1 + s_{11} \sigma_2 \quad .$$

Using the same fused silica fiber as mentioned in the text, in which $n_o = 1.5$, $D = .005$ in, s_{11} and s_{12} are 0.95 and -0.16 ($\times 10^{-7}$ in²/lb), respectively, with $F/L = 100$ lb/in, we calculated the following:

$$\text{At } x = y = 0: \quad \left. \begin{array}{l} \epsilon_1 = 1.8 \\ \epsilon_2 = -3.8 \end{array} \right\} \times 10^{-3}$$

$$\text{At } x = 0, y = \pm y_M: \left. \begin{array}{l} \epsilon_1 = 9.2 \\ \epsilon_2 = -47 \end{array} \right\} \times 10^{-3}$$

$$\text{At } x = 0, y = \pm D/2: \left. \begin{array}{l} \epsilon_1 = 2.7 \\ \epsilon_2 = -11 \end{array} \right\} \times 10^{-3}$$

$$\text{At } x = \pm D/2, y = 0: \epsilon_1 = \epsilon_2 = 0 \text{ because } \sigma_1 = \sigma_2 = 0$$

METRIC SYSTEM

BASE UNITS:

Quantity	Unit	SI Symbol	Formula
length	metre	m	...
mass	kilogram	kg	...
time	second	s	...
electric current	ampere	A	...
thermodynamic temperature	kelvin	K	...
amount of substance	mole	mol	...
luminous intensity	candela	cd	...

SUPPLEMENTARY UNITS:

Quantity	Unit	SI Symbol	Formula
plane angle	radian	rad	...
solid angle	steradian	sr	...

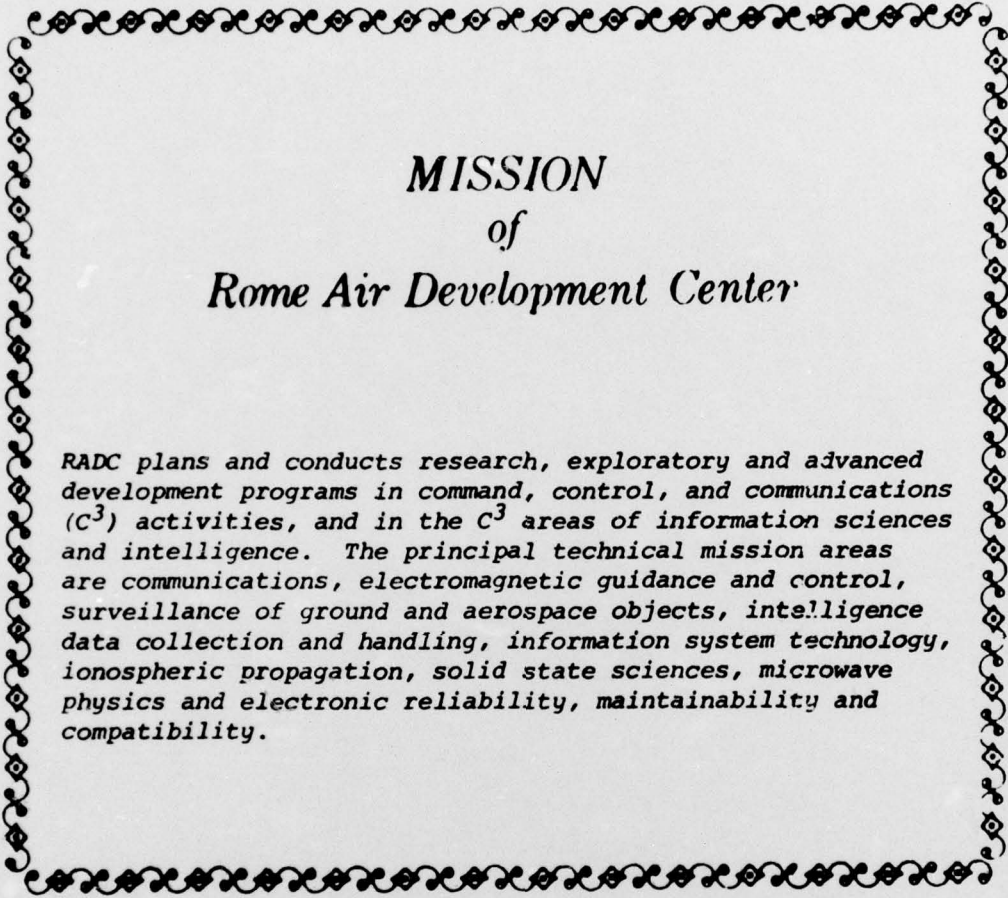
DERIVED UNITS:

Quantity	Unit	SI Symbol	Formula
Acceleration	metre per second squared	...	m/s ²
activity (of a radioactive source)	disintegration per second	...	(disintegration)/s
angular acceleration	radian per second squared	...	rad/s ²
angular velocity	radian per second	...	rad/s
area	square metre	...	m ²
density	kilogram per cubic metre	...	kg/m ³
electric capacitance	farad	F	A·s/V
electrical conductance	siemens	S	A/V
electric field strength	volt per metre	...	V/m
electric inductance	henry	H	V·s/A
electric potential difference	volt	V	W/A
electric resistance	ohm	Ω	V/A
electromotive force	volt	V	W/A
energy	joule	J	N·m
entropy	joule per kelvin	...	J/K
force	newton	N	kg·m/s ²
frequency	hertz	Hz	(cycle)/s
illuminance	lux	lx	lm/m ²
luminance	candela per square metre	...	cd/m ²
luminous flux	lumen	lm	cd·sr
magnetic field strength	ampere per metre	...	A/m
magnetic flux	weber	Wb	V·s
magnetic flux density	tesla	T	Wb/m ²
magnetomotive force	ampere	A	...
power	watt	W	J/s
pressure	pascal	Pa	N/m ²
quantity of electricity	coulomb	C	A·s
quantity of heat	joule	J	N·m
radiant intensity	watt per steradian	...	W/sr
specific heat	joule per kilogram-kelvin	...	J/kg·K
stress	pascal	Pa	N/m ²
thermal conductivity	watt per metre-kelvin	...	W/m·K
velocity	metre per second	...	m/s
viscosity, dynamic	pascal-second	...	Pa·s
viscosity, kinematic	square metre per second	...	m ² /s
voltage	volt	V	W/A
volume	cubic metre	...	m ³
wavenumber	reciprocal metre	...	(wave)/m
work	joule	J	N·m

SI PREFIXES:

Multiplication Factors	Prefix	SI Symbol
1 000 000 000 000 = 10 ¹²	tera	T
1 000 000 000 = 10 ⁹	giga	G
1 000 000 = 10 ⁶	mega	M
1 000 = 10 ³	kilo	k
100 = 10 ²	hecto*	h
10 = 10 ¹	deka*	da
0.1 = 10 ⁻¹	deci*	d
0.01 = 10 ⁻²	centi*	c
0.001 = 10 ⁻³	milli	m
0.000 001 = 10 ⁻⁶	micro	μ
0.000 000 001 = 10 ⁻⁹	nano	n
0.000 000 000 001 = 10 ⁻¹²	pico	p
0.000 000 000 000 001 = 10 ⁻¹⁵	femto	f
0.000 000 000 000 000 001 = 10 ⁻¹⁸	atto	a

* To be avoided where possible.



*MISSION
of
Rome Air Development Center*

RADC plans and conducts research, exploratory and advanced development programs in command, control, and communications (C³) activities, and in the C³ areas of information sciences and intelligence. The principal technical mission areas are communications, electromagnetic guidance and control, surveillance of ground and aerospace objects, intelligence data collection and handling, information system technology, ionospheric propagation, solid state sciences, microwave physics and electronic reliability, maintainability and compatibility.